AGU PUBLICATIONS

JGR

Journal of Geophysical Research: Space Physics

RESEARCH ARTICLE

10.1002/2013JA019623

Key Points:
- Alfvén wave is a possible source of strong IMF Bs
- AW-type Bs events are geoeffective
- AW-type Bs events are mainly in slow solar wind

Supporting Information:
- Readme
- Table S1

Correspondence to:
X.-Y. Zhang,
zhangxy@umich.edu

Citation:
Zhang, X.-Y., M. B. Moldwin, J. T. Steinberg, and R. M. Skoug (2014), Alfvén waves as a possible source of long-duration, large-amplitude, and geoeffective southward IMF, *J. Geophys. Res. Space Physics*, *119*, 3259–3266, doi:10.1002/2013JA019623.

Received 13 NOV 2013
Accepted 13 APR 2014
Accepted article online 15 APR 2014
Published online 16 MAY 2014

Alfvén waves as a possible source of long-duration, large-amplitude, and geoeffective southward IMF

X.-Y. Zhang[1], M. B. Moldwin[1], J. T. Steinberg[2], and R. M. Skoug[2]

[1]Department of Atmospheric, Oceanic, and Space Sciences, University of Michigan, Ann Arbor, Michigan, USA, [2]Los Alamos National Laboratory ISR-1 Group, Los Alamos, New Mexico, USA

Abstract The southward component (B_s) of the interplanetary magnetic field (IMF) is a strong driver of geomagnetic activity. Well-defined solar wind structures such as magnetic clouds and corotating interaction regions are the main sources of long-duration, large-amplitude IMF B_s. Here we analyze IMF B_s events ($t > 1$ h, $Bz < -5$ nT) unrelated with any well-defined solar wind structure at 1 AU using ACE spacecraft observations from 1998 to 2004. We find that about one third of these B_s events show Alfvénic wave features; therefore, those Alfvén waves in the solar wind are also an important source of long-duration, large-amplitude IMF southward component. We find that more than half of the Alfvén wave (AW)-related B_s events occur in slow solar wind (Vsw < 400 km/s). One third of the AW-type B_s events triggered geomagnetic storms, and half triggered substorms.

1. Introduction

The relationship between the interplanetary magnetic field (IMF) and the Earth's magnetospheric activities has been observationally studied extensively since *Fairfield and Cahill* [1966] found that the southward component of the IMF (IMF B_s) is associated with ground magnetic disturbances on Earth while the northward component corresponds to quiet geomagnetic conditions. The observation of IMF B_s is also evidence for solar coronal activity and provides a tool to study it [*Lindsay et al.*, 1999; *Hochedez et al.*, 2005]. Thus, IMF B_s is a key parameter to understand Sun-Earth relationship.

However, based on the classic Parker theory of the IMF alone [*Parker*, 1958], there is no meridional magnetic field component. In particular, for an observer in the ecliptic there is no significant, long-lasting component perpendicular to the ecliptic plane (e.g., IMF B_s) except for transients propagating outward from the Sun observed in the interplanetary medium as interplanetary coronal mass ejections (ICMEs) [*Klein and Burlaga*, 1982; *Lindsay et al.*, 1995], interplanetary small-scale magnetic flux ropes (ISMFRs) [*Moldwin et al.*, 2000; *Feng et al.*, 2010; *Zhang et al.*, 2012], and stream interaction regions (SIRs) [*Rosenberg and Coleman*, 1980].

In a recent study to understand the sources of IMF B_s, we defined IMF B_s events as continuous IMF B_s intervals with varying thresholds of B_s magnitude and duration and categorized their association with different solar wind structures, including magnetic clouds (MCs), ISMFRs, ICMEs without MC signature (ejecta), stream interacting regions (SIRs), and shocks, as well as events unrelated with well-defined solar wind structures [*Zhang and Moldwin*, 2014]. We found that for strong B_s events ($t > 1$ h, $Bz < -5$ nT, observed by WIND at 1 AU), ~28% were not associated with any well-defined solar wind structure shown in published event lists. The mystery about the source of these geoeffective, long-duration, large-amplitude B_s events that are not related with any well-defined solar wind structure motivates this study.

Alfvénic fluctuations represent another possible source of long-duration B_s in the solar wind. *Borovsky* [2008] presented a flux tube solar wind model in which the large spread in magnetic field orientations at 1 AU is due to a braiding of magnetic flux tubes about the Parker spiral direction. He suggested that the Alfvén-like discontinuities at the boundaries of the flux tube are due to reconnection at the foot of the flux tubes. *Tian et al.* [2010] also proposed that Alfvénic fluctuations are observed in periods consistent with flux rope signatures and called them Alfvén wave trains. It was also suggested that a torsional wave could be generated by distortions within a flux rope previously ejected from the Sun [*Gosling et al.*, 2010]. In contrast, turbulence in the solar wind [*Ragot*, 2006] or undamped Alfvén waves [e.g., *Burlaga et al.*, 1982] have also been proposed to be the source of angular variations of the solar wind magnetic field about the Parker spiral direction. These Alfvén fluctuations are the focus of this study.

Alfvén waves were first observed by *Coleman* [1967] based on comparison with an ideal, uniform solar wind model with a wide period range (10^2 to 5×10^4 s in the spacecraft frame) in the interplanetary medium. The cross helicity (Alfvén effect ratio) was first put forward by *Matthaeus and Goldstein* [1982] as one of the rugged invariants of 3-D ideal incompressible MHD turbulence theory. *Riley et al.* [1996] used this quantity to describe the "Alfvénicity," a measure of the correlation between variations of velocity and magnetic field. If the cross helicity is close to unity, the fluctuations of the solar wind are purely Alfvénic, and if it is close to zero, the fluctuations are non-Alfvénic; that is, the interplanetary medium is dominated by the convection of static structures [e.g., *Tu and Marsch*, 1992]. The Alfvén ratio was also introduced by *Matthaeus and Goldstein* [1982] to present the ratio between the kinetic and magnetic fluctuation energy. *Tu and Marsch* [1993] showed that as the heliocentric distance increases, the normalized cross helicity and Alfvén ratio decrease, from near 1 at 0.3 AU in high-speed solar wind to substantially less than 0.5 at 1 AU.

Alfvén waves are commonly observed in all types of solar wind flow [*Belcher and Davis*, 1971; *Tu and Marsch*, 1995, and references therein], and clearly, not all Alfvén waves lead to long-duration B_s events. However, this study of B_s events shows that some of these southward turnings are consistent with long-period Alfvén waves. Shorter-period Alfvén waves, small-amplitude waves, or waves which do not include strong fluctuations in the Z component obviously would not be able to generate the long-duration B_s field intervals which are the focus of this study.

Some previous studies have discussed the relationship between Alfvén waves and geomagnetic activity. In particular, Alfén waves within high-speed streams have been related to substorm activity [e.g., *Lee et al.*, 2006]. Also, *Tsurutani and Gonzalez* [1987] showed that the high-intensity ($AE > 1000$ nT), long duration ($T > 2$ days) continuous auroral activity (HILDCAA) events are induced by interplanetary Alfvén wave trains propagating outward from the Sun, primarily in observations following geomagnetic storms. Those authors suggested the HILDCAAs are caused by magnetic reconnection between the southward components of the Alfvén wave magnetic fields and magnetospheric fields.

In this study, we analyze the magnetic field and plasma data with 64 s resolution from the ACE spacecraft from 1995 to 2004 to study the detailed features of the IMF B_s events (duration > 1 h, $Bz < -5$ nT) that were considered to be unrelated with any well-defined solar wind structures [*Zhang and Moldwin*, 2014] based on previous published event lists.

2. Methodology

Zhang and Moldwin [2014] identified strong B_s events ($t > 1$ h, $Bz < -5$ nT) and associated them with well-defined solar wind structures using published event lists [*Jian et al.*, 2006b, 2011; *Zhang et al.*, 2012]. In this study, we examine the events that were found by *Zhang and Moldwin* [2014] to be unassociated with structures in the published lists. We examine the 64 s averaged ACE magnetic field and plasma data at 1 AU from 1995 to 2004 in order to study the source of these unassociated IMF B_s events ($t > 1$ h, $Bz < -5$ nT). We first use the ACE data to determine if there are solar wind structures (ICME, shocks, and SIR) present which were not captured by the published lists. For events which still show no association, we then look for Alfvén wave features.

Our methodology is as follows:

1. Because the previous study was performed using WIND data and the present analysis was performed using ACE, we compared the magnetic field data in GSE coordinates from WIND and ACE satellites to confirm that B_s events were seen with similar features by both satellites and to determine the boundary of the B_s event observed by ACE.
2. Examine the ion moments and superthermal electron (STEA) pitch angle data from ACE for features related to ICMEs, shocks, or SIRs during the intervals from (1) but not recognized in previous published lists; if the measured proton temperature is significantly lower than the expected temperature based on the solar wind speed during intervals not near the heliospheric current sheet [e.g., *Gosling et al.*, 1973; *Richardson and Cane*, 1995], or the STEA pitch angle in the energy channel of 272 eV shows a bidirectional distribution not associated with Earth's bow shock or a SIR [e.g., *Zwickl et al.*, 1983; *Gosling et al.*, 1987], this interval is categorized as an ICME; if there is a sharp increase of proton density, speed, temperature, and IMF magnitude, this event is considered shock associated; if there is a gradual increase of solar wind

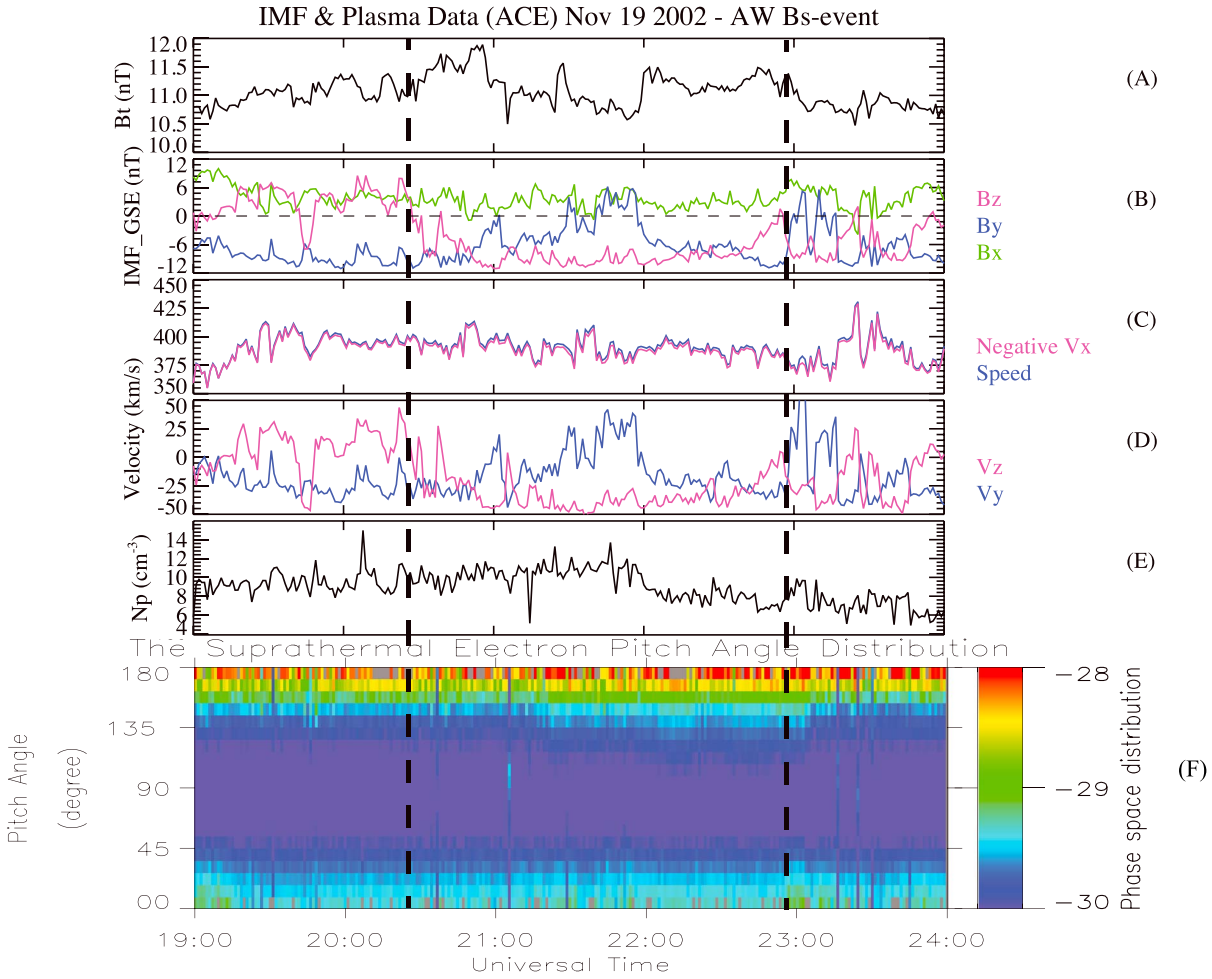

Figure 1. An example of an Alfvén wave-related B_s event observed by the ACE satellite at 1 AU. (a) Total interplanetary magnetic field (IMF) magnitude; (b) IMF *x*, *y*, and *z* components in GSE coordinates; (c) solar wind speed and negative *x* component of solar wind velocity in GSE coordinates; (d) *y* and *z* components of solar wind velocity in GSE coordinates; (e) solar wind proton density; and (f) suprathermal electron pitch angle distribution at 272 eV.

speed from the background average value (~ 400 km/s) to over 500 km/s, and decrease of proton density, the event is labeled as a SIR.

3. For the B_s events showing no features of ICME, shock, or SIR from (2), perform linear regression between the magnetic field and velocity field for the *x*, *y*, and *z* components in GSE coordinates; if the slopes of all three components have the same order (the difference between the largest and smallest value of slope is no more than 100%), this event is considered Alfvénic wave related; if one or two components change only slightly in both magnetic and velocity fields, while the other two or one components show a good linear relationship, this event is also categorized as Alfvén wave related. For further confirmation, we calculate the cross helicity and require it is > 0.5. If the fluctuation of the corresponding magnetic field and the velocity vectors have positive/negative correlation when the longitudinal angle of the IMF is negative/positive, the Alfvén wave is propagating outward; otherwise, it is inward.
4. Examine the geomagnetic activity indices (*SYM-H*, *AE*/*AU*/*AL*, and *PC*) starting from the same universal time of the Alfvén wave-related B_s event from (3) and ending 75 min later than the B_s event and compare with the results of our previous study [*Zhang and Moldwin*, 2014]. Based on the distribution of the averaged solar wind speed of the B_s events associated with Alfvén waves, we estimated the arrival time of slow solar wind from the Sun to the Earth and found that 75 min is enough to include the time shift and the magnetospheric response.

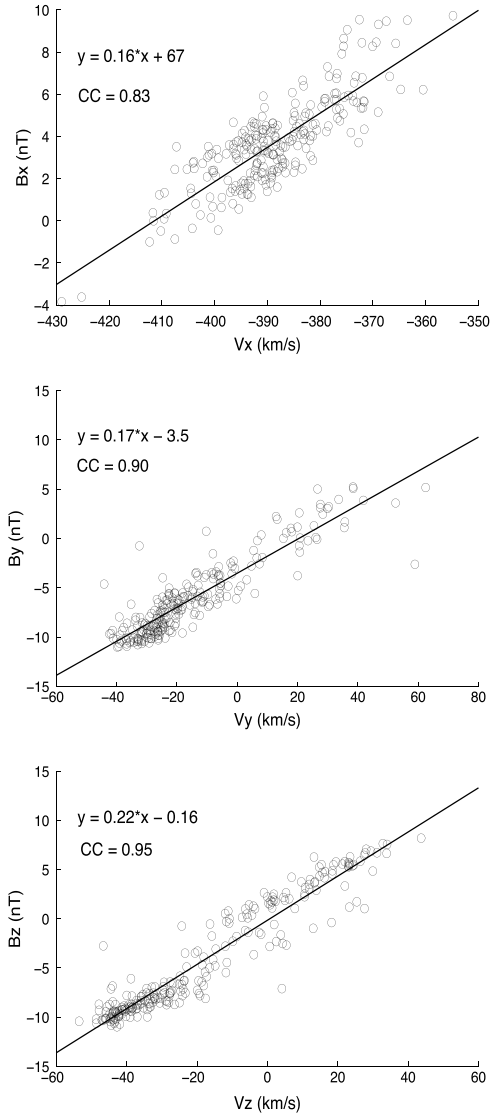

Figure 2. The linear regression of (top to bottom) *x*, *y*, and *z* components between magnetic field and velocity for the event shown in Figure 1. The scattered dots are observations from ACE, and the solid line shows the linear regression result. The equation and correlation coefficient of the linear regression are shown in each panel.

3. Results

Figure 1 gives an example of an Alfvén wave-related B_s event observed by the ACE satellite at 1 AU on 19 November 2002. The time period shown in the plot is 19:00–24:00 UT 19 November 2002, while the B_s event is from 20:30 to 22:50 UT marked by the dashed lines. During this B_s event, the magnitude of the total magnetic field and *Bx* did not change significantly but averaged about 11 and 3 nT, respectively. IMF *By* showed an increase from −5 nT to 5 nT during the first half of the B_s interval and then decreased to ∼ −10 nT until the end of this interval. Between the dashed lines in Figure 1c, the solar wind speed fluctuates around 390 km/s, while the component in the Sun-Earth direction varied simultaneously with the magnitude. It is seen from Figure 1d that there were sign changes of the *z* component of solar wind velocity in the same direction as the corresponding magnetic field component, which is also seen in the *y* component of both the magnetic field and solar wind velocity. We also examined the solar wind conditions over the solar rotation that covers this B_s event, showing that the solar wind speed remained around 400 km/s for 3 days before this event and a SIR occurred 2 days later. The pitch angle distribution of suprathermal electrons is peaked at 180°, that is antiparallel to the magnetic field over the whole interval, indicating an inward IMF sector.

Figure 2 shows the linear regression of the *x*, *y*, and *z* components (from top to bottom) between magnetic field and velocity for the event shown in Figure 1. The scattered dots are magnetometer and velocity observations from ACE, and the straight line shows the linear regression result. The equation and correlation coefficient of the linear regression are shown in each panel. The correlation coefficients for *x*, *y*, and *z* components are 0.83, 0.90, and 0.95, while the slopes are 0.16, 0.17, and 0.22, respectively. Combined with the fact that the longitude angle of the IMF during this interval almost stayed at −45°, the observations are consistent with Alfvén waves propagating antiparallel to the magnetic field, or antisunward within an inward polarity IMF sector. We also calculated the cross helicity as 0.78 for this B_s event (which is not shown in the plot).

Table 1. The Number of B_s Events (t > 1 h, Bz < −5 nT) During the Period of April 1998 to December 2004 in Each Category of Solar Wind Structures From Our Previous Study [*Zhang and Moldwin*, 2014] and the Current Study

	MC	Ejecta	SMFR	SIR	Shock	AW	Unidentified
Previous study [*Zhang and Moldwin*, 2014]	64	209	5	149	13	–	172
Current study	64	237	5	151	15	57	83

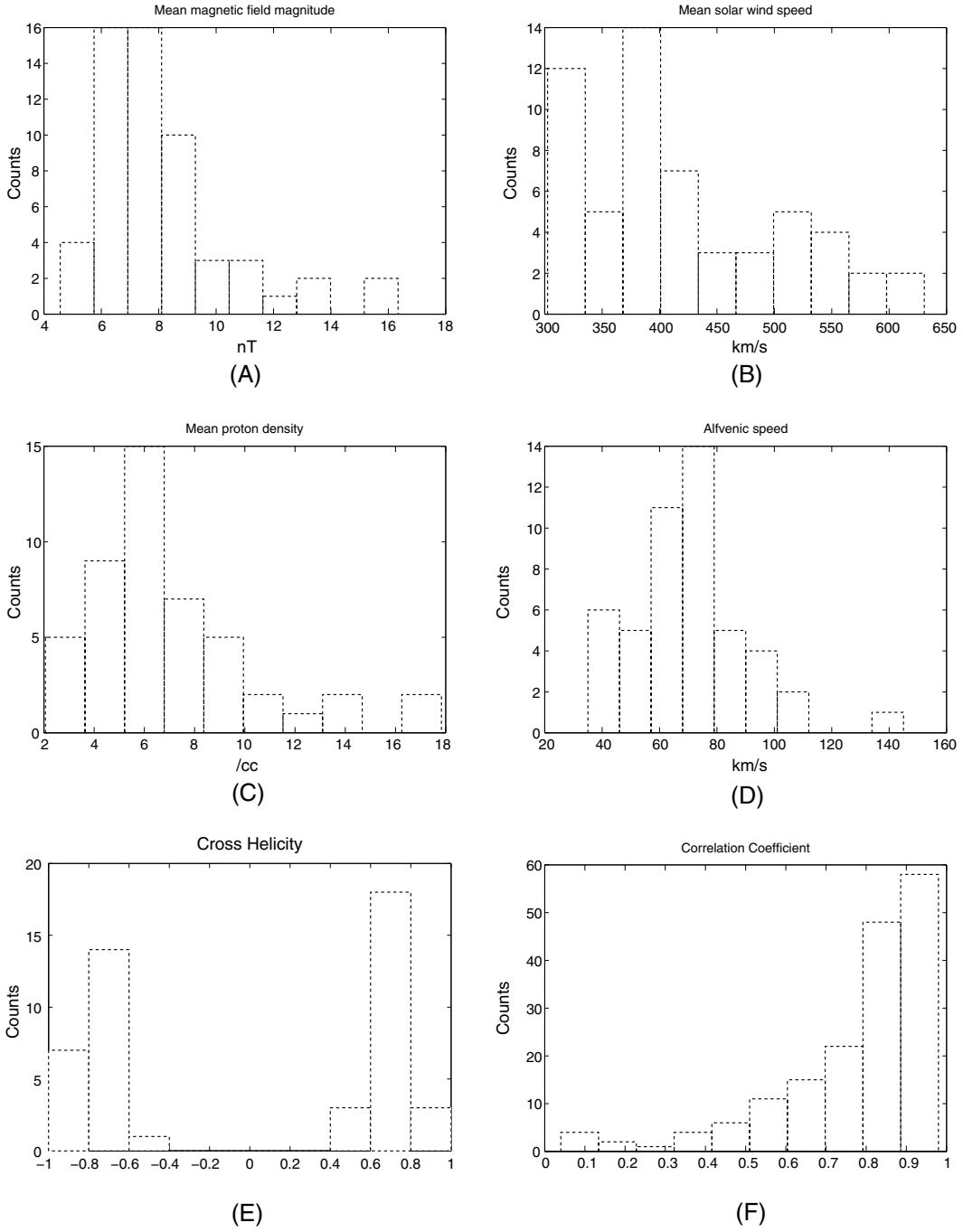

Figure 3. Histograms of mean values of the (a) IMF magnitude, (b) solar wind speed, (c) proton density, (d) Alfvénic speed, (e) cross helicity, and (f) correlation coefficient for the Alfvén wave-related B_s events.

We performed the above analysis on all of the unidentified events from the previous study. Table 1 shows the number of B_s events ($t > 1$ h, Bz < -5 nT) during the period of April 1998 to December 2004 in each category of solar wind structures from our previous study [*Zhang and Moldwin*, 2014] and the current study (event list included as supporting information). It shows that there are 28 B_s events identified as ejecta, two as SIRs, and two as shocks in this study that were not previously identified in published event lists. This study again finds that most B_s events are associated with ejecta, while about 10% of B_s events are associated with Alfvén waves where there are no other concurrent and predominant solar wind features. However, ~14% of B_s events are still not associated with any of these solar wind structures.

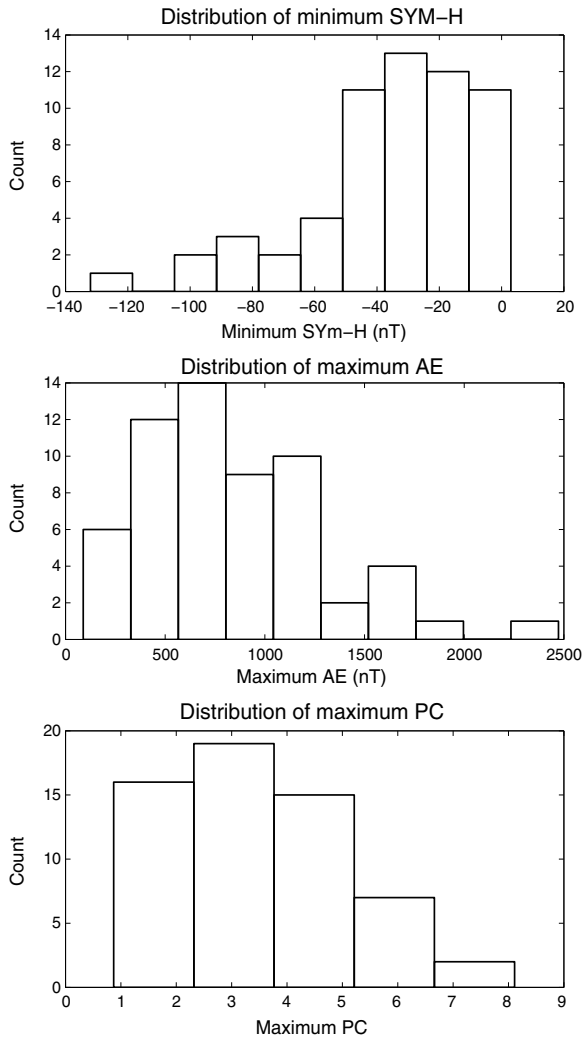

Figure 4. Histogram of minimum (top to bottom) *SYM-H* (nT), maximum *AE* (nT), and maximum *PC* for all the Alfvén wave-related B_s events (1998 April to 2004). The threshold of the duration and B_s magnitude of the B_s events are 1 h and 5 nT. The intervals of ground measurements start at the same universal time but end 75 min later than the B_s events observed by ACE.

Figure 3 shows the histograms of the properties of the 57 Alfvén wave-related B_s events. Figure 3a shows that for 62% of these B_s events, the average IMF magnitude is less than 8 nT but that five events have amplitudes greater than 12 nT. It is indicated from Figure 3b that only 22% of them propagated in solar wind with speed of more than 500 km/s, while over half of them occurred in solar wind with speed less than 400 km/s. The velocity distribution is peaked between 375 and 400 km/s. There are data gaps in proton density for nine events, so the total numbers of the counts in Figures 3c–3e are 48. The histogram in Figure 3c shows that three quarters of these events have mean proton density smaller than 8 cm^{-3}, with a most probable density of 6 cm^{-3}. Based on the measurements of magnetic field and proton density, we calculated the Alfvén speed (V_A) during the intervals shown in Figure 3d and found that 75% have V_A less than 80 km/s and peaked at V_A = 70–80 km/s. Using the definition of cross helicity [*Matthaeus and Goldstein*, 1982], we show in Figure 3e that the absolute value of the cross helicity is less than 0.6 for only one sixth of events and that the most frequent occurrence is at 0.8. We plot the correlation coefficients (CC) of the linear regression between the magnetic and velocity fields for all three components of all the 57 B_s events in Figure 3f. It is shown that about 74% of these intervals have CC higher than 0.7 between the two fields, which is an important criterion for identifying Alfvén waves in the solar wind.

Figure 4 shows the minimum *SYM-H* (nT), maximum *AE* (nT), and maximum polar cap index (*PC*) (from top to bottom) for all the Alfvén wave-related B_s events (1998 April to 2004). The intervals of ground measurements start at the same universal time as the Alfvénic events but end 75 mins later than the B_s events observed by ACE. The first panel shows that about one third of these events are followed by an interval of *SYM-H* less than −50 nT, indicating a geomagnetic storm. Around half of the events induce substorms, indicated by maximum *AE* greater than 1000 nT. The third panel of Figure 4 shows that more than half of these B_s events are related with *PC* index intervals larger than 4. *PC* index was proposed by *Troshichev et al.* [2011] to characterize the variability of the polar cap magnetic field. *Troshichev et al.* [1986, and references therein] suggested that *PC* ~ 2 is the threshold of a geomagnetic storm.

4. Discussions

Marsch and Tu [1990] analyzed the magnetic field and plasma data from the Helios spacecraft between 0.3 and 1 AU near the quiet phase of solar cycle 21 and found that in the solar wind fluctuations with frequency below 3×10^{-4} Hz are found in low-speed flows bordering the heliospheric current sheet and that the fluctuation spectrum at low frequencies drops much faster in fast streams than in slow streams. In this

study, we find that the distribution of the Alfvén wave (AW)-related B_s events duration is peaked at 2 h (7.2×10^3 s or 1.4×10^{-4} Hz in frequency), which is in the low-frequency range of Alfvén waves. As shown in Figure 3b, nearly 80% of these B_s events are embedded in solar wind slower than 500 km/s. We assume that the low-frequency Alfvén waves carrying long-duration, large-amplitude B_s intervals in this study originate as perturbations in the magnetic field on the Sun and propagate outward. If Alfvén waves in the solar wind have different source regions in the solar corona, which in turn affect their efficiency in accelerating the solar wind, the differences will be manifested in different spectra and plasma properties in the solar wind at farther heliocentric distance. For a future study, we will extend the observations to other spacecraft, such as STEREO and SOHO, and also combine with solar activity models to examine the source and evolution of the perturbations on the Sun.

In this study, we examine the B_s events not related with any well-defined solar wind structure in the previous *Zhang and Moldwin* [2014] study using the ACE magnetic field and plasma data from 1998 to 2004. There are often several features used to define a single solar wind phenomenon, but not all of the signatures always occur for every event, which makes it difficult to define a solar wind structure based on a fixed set of observational signatures. ICMEs in particular are very complex, with signatures such as bidirectional electrons, low proton temperatures, circularly polarized IMF, and enhanced alpha particle fluxes [e.g., *Moldwin et al.*, 1995; *Cane and Richardson*, 2003; *Jian et al.*, 2006b] often observed for only part of an event. This study identified some additional ICMEs from the IMF B_s events not previously associated with any well-defined solar wind structures [*Zhang and Moldwin*, 2014], based on the simultaneous occurrence of bidirectional suprathermal electrons and low proton temperature from ACE observations at 1 AU. Similar for SIRs, we identified additional SIRs based on the features of increasing solar wind flow speed and decreasing proton density. Previous studies [*Lindsay et al.*, 1995; *Jian et al.*, 2006a] have used other criteria to define a SIR, such as an increase of perpendicular solar wind dynamic pressure or increased temperature. We identified Alfvén waves as a source of long-duration, large-amplitude B_s intervals. Alfvén waves may be present in well-defined structures as well. We did not investigate that here. However, we did find that at times, Alfvén waves are the only apparent reason for southward turning of the field. There are still B_s events not related to either solar wind structures or Alfvénic features that need more detailed study in the future.

We analyzed the storm activity index *SYM-H* and found that about one third of the AW-type B_s events triggered storms (*SYM-H* < -50 nT). However, compared to B_s events in other categories, the AW-type B_s events are a weaker source for triggering geomagnetic storms. During the B_s events ($t > 1$ h, $Bz < -5$ nT) categorized by *Zhang and Moldwin* [2014] and this study from April 1998 to end of 2004, 123 storms occurred, 40% due to ICMEs, 44% due to SIRs, 5% by shocks, 1% by SMFR, and 10% due to AWs. The differences of the contribution to triggering magnetic storms among different solar wind structure-related B_s events are their occurrence frequency and average solar wind speed [*Zhang and Moldwin*, 2014]. While AW-type B_s events are geoeffective, it is hard to forecast the occurrence of these B_s intervals based on coronagraph observations several days in advance. Thus, we need to study the mechanisms of the magnetic activity on the Sun and how magnetic structures evolve in transit to the Earth using multispacecraft observations and models.

5. Conclusions

In this study, Alfvén wave (AW)-related B_s events are defined primarily based on the linear correlation between the magnetic field and velocity components and verified by the cross helicity. We also present the geomagnetic field response to IMF B_s events related with Alfvén waves to analyze their geoeffectiveness. We find that some long-duration, large-amplitude B_s intervals are identified as Alfvén waves in slow solar wind. Perturbations on the Sun propagating outward may be the source of these low-frequency Alfvén waves. We find that these AW-type B_s events are geoeffective but produce weaker geomagnetic response than ICME- and SIR-related B_s events. However, it is very difficult to predict the occurrence of Alfvén waves and their geoeffectiveness from coronagraph images or other solar images. Although this study demonstrates an additional source of long-duration, large-amplitude IMF southward component, there are still long-duration, large-amplitude B_s events with complex signatures in the magnetic field and plasma parameters not associated with solar wind structures needing further study to attempt to determine their source.

Acknowledgments
This work was supported by NASA NESSF grant NNX13AM35H. Work at Los Alamos was performed under the auspices of the U.S. Department of Energy, with support from the NASA ACE program and the Los Alamos Space Weather Summer School (2013).

Philippa Browning thanks the reviewers for their assistance in evaluating this paper.

References

Belcher, J. W., and L. Davis (1971), Large-amplitude Alfvén waves in the interplanetary medium, 2, *J. Geophys. Res.*, *76*, 3534–3563.
Borovsky, J. E. (2008), Flux tube texture of the solar wind: Strands of the magnetic carpet at 1 AU?, *J. Geophys. Res.*, *113*, A08110, doi:10.1029/2007JA012684.
Burlaga, L. F., R. P. Lepping, and K. W. Behannon (1982), Large-scale variations of the interplanetary magnetic field: Voyager 1 and 2 observations between 1-5 AU, *J. Geophys. Res.*, *87*, 4345–4353.
Cane, H. V., and I. G. Richardson (2003), Interplanetary coronal mass ejections in the near-Earth solar wind during 1996–2002, *J. Geophys. Res.*, *108*(A4), 1156, doi:10.1029/2002JA009817.
Coleman, P. J. (1967), Wave-like phenomena in the interplanetary plasma: Mariner 2, *Planet. Space Sci.*, *15*, 953–973.
Fairfield, D. H., and J. L. J. Cahill (1966), Transition region magnetic field and polar magnetic disturbances, *J. Geophys. Res.*, *71*(1), 155–169.
Feng, H.-Q., J.-K. Chao, L. H. Lyu, and L. C. Lee (2010), The relationship between small interplanetary magnetic flux rope and the substorm expansion phase, *J. Geophys. Res.*, *115*, A09108, doi:10.1029/2009JA015191.
Gosling, J. T., V. Pizzo, and S. J. Bame (1973), Anomalously low proton temperature in the solar wind following interplanetary shock waves—Evidence for magnetic bottles?, *J. Geophys. Res.*, *78*, 2001–2009.
Gosling, J. T., D. N. Baker, S. J. Bame, W. C. Feldman, R. D. Zwickl, and E. J. Smith (1987), Bidirectional solar wind electron heat flux events, *J. Geophys. Res.*, *92*, 8519–8535.
Gosling, J. T., W.-L. Teh, and S. Eriksson (2010), A torsional Alfvén wave embedded within a small magnetic flux rope in the solar wind, *The Astrophys. J.*, *719*, L36.
Hochedez, J.-F., A. Zhukov, E. Robbrecht, R. V. der Linden, D. Berghmans, P. Vanlommel, A. Theissen, and F. Clette (2005), Solar weather monitoring, *Ann. Geophys.*, *23*, 3149–3161.
Jian, L. K., C. Russell, J. G. Luhmann, and R. M. Skoug (2006a), Properties of stream interactions at one AU during 1995–2004, *Sol. Phys.*, *239*, 337–392.
Jian, L. K., C. Russell, J. G. Luhmann, and R. M. Skoug (2006b), Properties of interplanetary coronal mass ejections at one AU during 1995–2004, *Sol. Phys.*, *239*, 393–436.
Jian, L. K., C. Russell, J. G. Luhmann, P. J. MacNeice, D. Odstricil, P. Riley, J. A. Linker, R. M. Skoug, and J. T. Steinberg (2011), Comparison of observations at ACE and Ulysses with Enlil model results: Stream interaction regions during Carrington rotations 2016–2018, *Sol. Phys.*, *273*, 179–203.
Klein, L. W., and L. F. Burlaga (1982), Interplanetary magnetic clouds at 1 AU, *J. Geophys. Res.*, *87*, 613–624.
Lee, D., et al. (2006), Repetitive substorms caused by Alfvénic waves of the interplanetary magnetic field during high-speed solar wind streams, *J. Geophys. Res.*, *111*, A12214, doi:10.1029/2006JA011685.
Lindsay, G. M., C. T. Russell, and J. G. Luhmann (1995), Coronal mass ejection and stream interaction region characteristic and their potential geomagnetic effectiveness, *J. Geophys. Res.*, *10*, 16,999–17,013.
Lindsay, G. M., J. G. Luhmann, C. T. Russell, and J. T. Gosling (1999), Relationships between coronal mass ejection speeds from coronagraph images and interplanetary characteristics of associated interplanetary coronal mass ejections, *J. Geophys. Res.*, *104*, 12,515–12,523.
Marsch, E., and C.-Y. Tu (1990), Spectral and spatial evolution of compressible turbulence in the inner solar wind, *J. Geophys. Res.*, *95*, 11,945–11,956.
Matthaeus, W. H., and M. L. Goldstein (1982), Measurement of the rugged invariants of magnetohydrodynamic turbulence in the solar wind, *J. Geophys. Res.*, *87*, 6011–6028.
Moldwin, M. B., J. L. Phillips, J. T. Gosling, E. E. Scime, D. J. McComas, and S. J. Bame (1995), Ulysses observation of a noncoronal mass ejection flux rope: Evidence of interplanetary magnetic reconnection, *J. Geophys. Res.*, *100*, 19,903–19,910.
Moldwin, M. B., S. Ford, R. Lepping, J. Slavin, and A. Szabo (2000), Small-scale magnetic flux ropes in the solar wind, *Geophys. Res. Lett.*, *27*, 57–60.
Parker, E. N. (1958), Dynamics of the interplanetary gas and magnetic fields, *The Astrophys. J.*, *128*, 664.
Ragot, B. R. (2006), Distribution of magnetic field orientations in the turbulent solar wind, *The Astrophys. J.*, *651*, 1209–1218.
Richardson, I. G., and H. V. Cane (1995), Regions of abnormally low proton temperature in the solar wind (1965–1991) and their association with ejecta, *J. Geophys. Res.*, *100*, 23,397–23,412.
Riley, P., C. P. Sonett, B. T. Tsurutani, A. Balogh, R. J. Forsyth, and G. W. Hoogeveen (1996), Properties of arc-polarized Alfvén waves in the ecliptic plane: Ulysses observations, *J. Geophys. Res.*, *101*, 19,987–19,993.
Rosenberg, R. L., and J. P. J. Coleman (1980), Solar cycle-dependent north-south field configurations observed in solar wind interaction regions, *J. Geophys. Res.*, *85*, 3021–3032.
Tian, H., Y. Shuo, Q.-G. Zong, J.-S. He, and Q. Yu (2010), Signatures of magnetic reconnection at boundaries of interplanetary small-scale magnetic flux ropes, *The Astrophys. J.*, *720*, 454–464.
Troshichev, O. A., A. L. Kotikov, B. D. Bolotinskaya, and V. G. Andresen (1986), Influence of the IMF azimuthal component on magnetospheric substorm dynamics, *J. Geomagn. Geoelec.*, 1075–1088.
Troshichev, O. A., D. Sormakov, and A. Janzhura (2011), Relation of PC index to the geomagnetic storm Dst variation, *J. Atmos. Sol. Terr. Phys.*, *73*, 611–622.
Tsurutani, B. T., and W. D. Gonzalez (1987), The cause of high intensity long-duration continuous AE activity (HILDCAAs): Interplanetary Alfvén wave trains, *Planet. Space Sci.*, *35*, 405–412.
Tu, C.-Y., and E. Marsch (1992), The evolution of MHD turbulence in the solar wind, in *Solar Wind Seven*, edited by E. Marsch and R. Schwenn, pp. 549–554, Pergamon Press, Oxford, U. K.
Tu, C.-Y., and E. Marsch (1993), A model of solar wind fluctuations with two components: Alfvén waves and convective structures, *J. Geophys. Res.*, *98*, 1257–1276.
Tu, C.-Y., and E. Marsch (1995), MHD structures, waves and turbulence in the solar wind: Observations and theories, *Space Sci. Rev.*, *73*, 1–210.
Zhang, X.-Y., and M. B. Moldwin (2014), The source, statistical properties and geoeffectiveness of long-duration southward interplanetary magnetic field intervals, *J. Geophys. Res. Space Physics*, *119*, 658–669, doi:10.1002/2013JA018937.
Zhang, X.-Y., M. B. Moldwin, and M. Cartwright (2012), The geo-effectiveness of interplanetary small-scale magnetic flux ropes, *J. Atmos. Sol. Terr. Phys.*, *95-96*, 1–14.
Zwickl, R. D., J. R. Asbridge, S. J. Bame, W. C. Feldman, J. T. Gosling, and E. J. Smith (1983), Plasma properties of driver gas following interplanetary shocks observed by ISEE-3, in *Solar Wind Five*, edited by M. Neugebauer, NASA Conf. Publ., 2280, 711.